

1 Pollen dispensing schedules in buzz-pollinated plants: Experimental
2 comparison of species with contrasting floral morphologies

3

4 Jurene E. Kemp^{1,*}

5 Mario Vallejo-Marín¹

6

7 ¹Department of Biological and Environmental Sciences, University of Stirling. Stirling, Scotland,
8 United Kingdom, FK9 4LA.

9

10 *Author for correspondence:

11 Email: jurenekemp@yahoo.com

12

13 Manuscript received _____; revision accepted _____.

14

15 Running title: Pollen dispensing schedules in buzz-pollinated plants

16

This is the peer reviewed version of the following article: Kemp, J. E., and Vallejo-Marín, M.. 2021. Pollen dispensing schedules in buzz-pollinated plants: experimental comparison of species with contrasting floral morphologies. *American Journal of Botany* 108(6): 993– 1005, which has been published in final form at <https://doi.org/10.1002/ajb2.1680>. This article may be used for non-commercial purposes in accordance with Wiley Terms and Conditions for self-archiving.

17 ABSTRACT

18 Premise: Plants can mitigate the fitness costs associated with pollen consumption by floral
19 visitors by optimizing pollen release rates. In buzz-pollinated plants, bees apply vibrations to
20 remove pollen from anthers with small pores. These poricidal anthers potentially function as
21 mechanism staggering pollen release, but this has rarely been tested across plant species
22 differing in anther morphology.

23 Methods: In *Solanum* section *Androceras*, three pairs of buzz-pollinated species have undergone
24 independent evolutionary shifts between large- and small-flowers, which are accompanied by
25 replicate changes in anther morphology. We used these shifts in anther morphology to
26 characterise the association between anther morphology and pollen dispensing schedules. We
27 applied simulated bee-like vibrations to anthers to elicit pollen release, and compared pollen
28 dispensing schedules across anther morphologies. We also investigated how vibration velocity
29 affects pollen release.

30 Key Results: Replicate transitions in *Solanum* anther morphology are associated with consistent
31 changes in pollen dispensing schedules. We found that small-flowered taxa release their pollen
32 at higher rates than their large-flowered counterparts. Higher vibration velocities resulted in
33 quicker pollen dispensing and more total pollen released. Finally, both the pollen dispensing rate
34 and the amount of pollen released in the first vibration were negatively related to anther wall
35 area, but we did not observe any association between pore size and pollen dispensing.

36 Conclusions: Our results provide the first empirical demonstration that the pollen dispensing
37 properties of poricidal anthers depend on both floral characteristics and bee vibration
38 properties. Morphological modification of anthers could thus provide a mechanism to exploit
39 different pollination environments.

40

41 **Key words:** buzz pollination, biomechanics, pollen presentation theory, poricidal anther morphology,
42 *Solanum*, sonication.

43 INTRODUCTION

44 Most flowering plant species rely on animals to transport pollen between conspecific flowers for
45 fertilisation (Ollerton et al., 2011). Despite the widespread reliance on animals as pollen vectors,
46 animal pollination can limit pollen dispersal, particularly when visitors actively collect pollen, making
47 it unavailable for fertilisation (Harder and Wilson, 1994; Minnaar et al., 2019). In nectarless plants,
48 where pollen serves both pollinator reward and vehicles for male gametes, we expect selection to
49 favour adaptations that limit the fitness costs associated with pollen consumption, whilst releasing
50 enough pollen to ensure sufficient pollinator visits (Harder and Thomson, 1989; Harder and Barclay,
51 1994; LeBuhn and Holsinger, 1998; Vallejo-Marín et al., 2009). Plants can theoretically mitigate the
52 fitness costs associated with pollen consumption by optimizing their pollen dispensing schedules
53 (i.e., the rate at which pollen is released across visits) to the visitation rates and grooming
54 behaviours of pollinators (Harder and Thomson, 1989; Harder and Wilson, 1994; LeBuhn and
55 Holsinger, 1998).

56 Theoretical models predict that pollen should be gradually released across multiple visits
57 when pollinator visits are unlimited and when their grooming behaviours result in high diminishing
58 fitness returns (i.e., when the total amount of pollen transferred decreases with the amount of
59 pollen collected per visit) (Harder and Thomson, 1989; Harder and Wilson, 1994). In contrast, when
60 pollinator visits are limited and have high per-visit transfer efficiencies, pollen should be released
61 across fewer visits (Harder and Thomson, 1989; Harder and Wilson, 1994). Thus, when pollinators
62 collect pollen and exhibit low per-visit transfer efficiencies, as in many bee pollinated taxa, models
63 predict that selection will favour pollen being gradually released across multiple visits if pollinators
64 are abundant (Thomson, 1986; Harder and Thomson, 1989; Holsinger and Thomson, 1994;
65 Schlindwein et al., 2005; Harder and Johnson, 2009). However, restricting pollen removal excessively
66 might be in conflict with the requirements of pollinators that collect pollen, and pollinators might
67 avoid visiting flowers that release too little pollen per visit (Harder, 1990). Pollen dispensing
68 schedules thus represent the evolutionary outcome of selective pressures acting on plants and
69 mediated by pollinators, and are particularly important in plants that offer pollen as the primary
70 reward (Harder and Barclay, 1994).

71 Plants can dispense pollen gradually through moderating anther maturation within a flower or
72 by staggering flower opening within a plant individual (Sargent, 2003; Castellanos et al., 2006a; Li et
73 al., 2014). Another potential solution to limit per-visit pollen collection is to physically restrict access
74 to pollen, as is done in poricidal anthers that contain pollen inside the anthers (Buchmann et al.,
75 1977; Harder and Barclay, 1994; Dellinger, Pöllabauer, et al., 2019). Poricidal anthers are associated

76 with buzz-pollination (Buchmann, 1983). During buzz pollination, bees vibrate flowers using their
77 thoracic muscles. The vibrations transmitted through the anthers cause pollen to be ejected through
78 the apical pores (De Luca and Vallejo-Marín, 2013; Vallejo-Marín, 2019). Buzz-pollinated flowers are
79 typically nectarless and solely offer pollen as reward (Buchmann, 1983; Faegri, 1986; Vallejo-Marín
80 et al., 2010), which makes them a likely candidate for gradual pollen release. Buzz-pollination is
81 widespread among plants, with more than 20,000 species possessing poricidal anthers (Buchmann,
82 1983), and about half of bee species capable of producing floral vibrations (Buchmann, 1983;
83 Cardinal et al., 2018). The floral and anther morphology of buzz-pollinated flowers is very diverse,
84 and even plants with poricidal anthers vary widely in their stamen morphology, both between and
85 within species (Buchmann, 1983; Dulberger et al., 1994; Corbet and Huang, 2014; Vallejo-Marín et
86 al., 2014; Dellinger, Artuso, et al., 2019; Dellinger, Chartier, et al., 2019). Similarly, the vibration
87 properties of bees vary across and within species (King and Buchmann, 2003; Arceo-Gómez et al.,
88 2011; Corbet and Huang, 2014; Arroyo-Correa et al., 2019; De Luca et al., 2019; Pritchard and
89 Vallejo-Marín, 2020), and previous empirical work demonstrates that vibration properties,
90 particularly their amplitude, affect pollen release (Harder and Barclay, 1994; King and Buchmann,
91 1996; De Luca et al. 2013). However, we know relatively little about how plant species with different
92 anther and floral morphologies vary in their pollen release schedules (but see Harder and Barclay
93 1994, Dellinger et al. 2019), including their response to vibrations of different amplitudes.

94 Anther properties, such as shape, length, natural frequency and pore size, are theoretically
95 expected to influence pollen release (Buchmann and Hurley, 1978; Vallejo-Marín et al., 2009). In
96 what remains the only biophysical model of buzz pollination, Buchmann and Hurley (1978), modelled
97 a poricidal anther with a simple geometry (a rectangular box) and an anther pore at one end. The
98 anther vibrates along a single spatial axis perpendicular to the longest anther dimension, with pollen
99 grains bouncing against the interior walls of the anther locule. In this model, pollen release occurs
100 when the kinetic energy of the vibrating anthers is transferred to the pollen grains, which are then
101 ejected through the pore. The higher the energy, the higher the pollen release rate. Pollen grains can
102 gain energy as they bounce against the interior of the anther walls or against each other. Thus, the
103 internal surface area of the anther locule along the axis of vibration (A) is positively related with the
104 rate of change in energy of pollen grains (equation 9 in Buchman and Hurley, 1978). However,
105 energy can also be lost as pollen grains escape the anther through the pore, and therefore the area
106 of the anther pore (A') is negatively related to changes in pollen energy (eqn. 9). Because A' is
107 positively related to the rate at which pollen grains are released from anthers (equation 10), but
108 negatively related to changes in pollen's kinetic energy, the relationship between anther pore size
109 and pollen release dynamics is not immediately obvious, as dynamics change as the anther empties

110 while vibrated. Numerical integration of Buchman and Hurley’s model suggests that both increased
111 anther wall area and pore size should result in faster times to empty anthers, and larger anther
112 volumes should result in slower pollen release (B. Travacca and M. Vallejo-Marín, unpublished), but
113 clearly more theoretical work is needed in this area.

114 In contrast to the absence of work on associations between anther morphology and pollen
115 release rates, the effect of the type of vibration applied (e.g., vibration frequency, amplitude and
116 duration) on pollen release has received more attention (Harder and Barclay, 1994; De Luca et al.,
117 2013; Rosi-Denadai et al., 2018). A study using bee-like vibrations (in terms of frequency, duration
118 and amplitude) showed that pollen release is more strongly affected by amplitude and duration than
119 by the frequency of the vibration (De Luca et al., 2013). However, previous studies assessing the
120 effects of vibration properties on pollen release have focused on the amount of pollen released
121 during a single vibration, and thus it has not been possible to build a full picture of pollen release
122 curves following multiple consecutive buzzes.

123 Here, we characterise pollen dispensing schedules across three pairs of closely related buzz-
124 pollinated taxa in the genus *Solanum* section *Androceras* (Solanaceae). These six taxa represent
125 three pairs of independent evolutionary transitions from large flowers with large anthers and small
126 pores, to small flowers with small anthers and large pores (Whalen 1978; 1979; Vallejo-Marin et al.,
127 2014; Rubini-Pisano et al., in prep). These large- to small-flower transitions bear the classic hallmark
128 traits of shifts in mating system from outcrossing towards increased self-pollination (Vallejo-Marín et
129 al., 2014; Rubini-Pisano et al., in prep), but have also been suggested to be associated with pollinator
130 shifts (Whalen, 1978). Regardless of the cause of the shift in flower and anther morphology, these
131 changes allow us to investigate the association between anther morphology and pollen dispensing
132 schedules in closely related taxa. We first investigate whether these replicate transitions in general
133 floral morphology are associated with replicate changes in pollen dispensing schedules. We then use
134 one of these evolutionary transitions from large- to small-flowered species to investigate the extent
135 to which pollen dispensing schedules depend on vibration velocity. Finally, we test whether the
136 parameters in the Buchmann and Hurley (1978) model can predict pollen release rates in the six
137 focal taxa. The replicate evolutionary transitions in anther morphology in three closely related clades
138 of *Solanum* provide an ideal opportunity to establish how pollen dispensing schedules of buzz-
139 pollinated plants vary with anther morphology, and how this is influenced by vibration properties.

140 MATERIALS AND METHODS

141 ***Study system-***

142 *Solanum* (Solanaceae) is often used as a model system for studying buzz-pollination (Vallejo-Marín
143 2019). This genus contains c. 1,350 species with nectarless flowers, representing about half of the
144 species diversity in the family Solanaceae (Särkinen et al., 2013). *Solanum* flowers are pentamerous,
145 usually radially symmetric, and bear poricidal anthers (Harris, 1905; Knapp, 2002). During buzz-
146 pollination, bees typically grab the base of the anthers using their mandibles whilst curling the
147 ventral side of their bodies around the anthers. They then use their indirect flight muscles to vibrate
148 the anthers to instigate pollen release (King et al., 1996). *Solanum* section *Androceras* is a
149 monophyletic clade consisting of approximately 12 annual and perennial species distributed in
150 Mexico and the southern USA (Whalen, 1978; Stern et al., 2010). All taxa in section *Androceras* are
151 heterantherous, i.e., have two or more morphologically differentiated sets of anthers in the same
152 flower. In heterantherous species, one set of anthers is usually associated with pollinator attraction
153 and reward (“feeding” anthers), while the other set contributes disproportionately to fertilising
154 ovules (“pollinating” anthers) (Vallejo-Marín et al., 2009). The section is divided into three series:
155 *Androceras*, *Pacificum*, and *Violaceiflorum* (Whalen, 1979). Parallel shifts in flower and anther
156 morphology have occurred within each of these three series (Vallejo-Marín et al., 2014) (Figs. 1 & 2).
157 In series *Androceras*, *S. rostratum* has large flowers, and long anthers with small anther pores,
158 whereas *S. fructu-tecto* has small flowers with small anthers and large anther pores (referred to as
159 the SR-SF clade, hereafter). Similar morphological shifts are present in series *Pacificum* for *S. grayi*
160 var. *grandiflorum* (large flowers) and *S. grayi* var. *grayi* (small flowers) (referred to as the SGN-SGG
161 clade, hereafter), and in series *Violaceiflorum* for *S. citrullifolium* (large flowers) and *S. heterodoxum*
162 (small flowers) (referred to as the SC-SH clade hereafter). These shifts in floral morphology is
163 potentially associated with shifts in mating system (i.e., from outcrossing to selfing), although this
164 has not been empirically confirmed (Vallejo-Marín et al., 2014). Within these species pairs, the
165 pollinating and feeding anthers are less differentiated in the small flower types than in the large
166 flower types (Vallejo-Marín et al., 2014). We refer to these two distinct floral morphologies as the
167 ‘small flower type’ and ‘large flower type’ throughout.

168 ***Seed collection and plant growth-***

169 Seeds were collected from natural populations in Mexico between 2007 and 2010, except for *S.*
170 *citrullifolium* which was obtained from the Solanaceae collection at Radboud University, Netherlands
171 (Experimental Garden and Genebank Solanaceae collection). For each plant species, we used seeds
172 from a single population. Accession numbers and sample localities are provided in Appendix S1 (see
173 Supplemental Data with this article). Germination was induced by treating seeds for 24h with 1000
174 ppm aqueous solution of gibberellic acid (GA3; Sigma-Aldrich, Dorset, UK), following the method of
175 Vallejo-Marín et al. (2014). Two to four weeks after germination, seedlings were transplanted to 1.5

176 L pots and kept in a pollinator-proof greenhouse with natural light supplemented with compact
177 fluorescent lamps to provide at least 16hours of daylight. Supplemental heating was provided to
178 maintain minimum temperatures above 16°C (night) and 25°C (day).

179 ***Synthesising bee-like vibrations and playback system-***

180 To characterise pollen dispensing schedules, we applied mechanical vibrations to flowers. We used
181 Audacity v2.1.3 (<http://audacity.source-forge.net/>) to generate an artificial vibration (stimulus) with
182 similar frequency properties to the vibrations that bees produce when extracting pollen (De Luca
183 and Vallejo-Marín, 2013). The vibrations consisted of a pure tone (300 Hz) sine wave made of five
184 consecutive pulses of 200 milliseconds (ms) each with 200 ms of silence between pulses (i.e., total
185 stimulus length = 2 seconds). Each pulse had a fade-in feature of 10 ms (Appendix S2). Multiple short
186 buzzes with a single dominant frequency characterise the floral vibrations of buzz pollinating bees
187 (De Luca and Vallejo-Marín, 2013, Pritchard and Vallejo-Marín, 2020), and a 300 Hz frequency was
188 selected to capture the frequency of floral vibrations typically produced by medium-sized bees,
189 including bumblebees (De Luca and Vallejo-Marín, 2013; Switzer and Combes, 2017; Arroyo-Correa
190 et al., 2019; De Luca et al., 2019; Pritchard and Vallejo-Marín, 2020). Previous studies have shown
191 that variation in frequency does not alter pollen release in a single vibration, but rather, higher
192 accelerations result in higher pollen release (De Luca et al., 2013). Theoretically, if flowers are
193 vibrated at the natural frequency of anthers, higher pollen release could be induced due to the
194 higher accelerations associated with resonance (King and Buchmann, 1996). For our six taxa, Nunes
195 (2020) showed that only the feeding anthers of *S. grayi grayi* might resonate at 300 Hz (mean
196 natural frequency = 294 Hz). We thus used a single ecologically relevant frequency for all
197 experiments (i.e. 300 Hz), and we vary acceleration in the experiments (described below). The
198 vibration amplitude was calibrated as described below to obtain the appropriate velocity for each
199 experiment.

200 The synthesised vibrations were applied using a custom-made vibration transducer system
201 (A. Gordon and M. Vallejo-Marín, unpublished; Appendix S3). This playback system consisted of a
202 vibration transducer speaker (Adin S8BT 26W, Shenzhen, China) with a vibrating metal plate. We
203 attached a metal rod (15 cm long with a 0.5 cm diameter) using an ethyl cyanoacrylate glue (Loctite
204 UltraGel Control, Düsseldorf, Germany) and plastic supports at the base. We fixed a pair of
205 featherlight forceps (D4045, Watkins & Doncaster, Leominster, UK) to the distal end of the metal rod
206 at a 90° angle using a metal clip. We used laser vibrometry to calibrate the vibration amplitude and
207 check that the playback frequency matched the input frequency. Briefly, we deployed a PDV-100
208 laser vibrometer (PDV-100, Polytec, Waldbronn, Germany) and focused the laser close to the tip of

209 the forceps (~1 cm from the tip), where we had placed a small amount of reflective tape. The laser
210 beam was aimed on the forceps perpendicular to the main axis of displacement of the transduction
211 system. The vibration signal was played in Audacity using a laptop computer connected to the
212 transduction system. The frequency and amplitude of the vibration was checked using VibSoft-20
213 data acquisition and software (Polytec, Waldbronn, Germany). Peak amplitude velocity of the
214 vibration was adjusted using the volume control in the computer until the desired velocity was
215 obtained. This calibration was done at the beginning of every day of the experiment, and again after
216 pollen was extracted from 3-5 flowers.

217 ***Pollen extraction and counting-***

218 Experimental flowers were brought from the glasshouse between 7h00 and 9h00 on the first day of
219 flower opening in a closed container with wet floral foam (Oasis Floral Products, Washington, UK), to
220 prevent flowers from drying out. Closed flower buds were tagged on the previous day in the late
221 afternoon to ensure that only newly opened flowers are used in the experiments. All pollen
222 extraction treatments were done within three hours after the flowers were picked. Maximum ten
223 flowers were used per day, depending on availability, and multiple plant species were used each
224 day. The artificial stimuli were applied to flowers in May 2019 at room temperature (22°C) in an
225 indoor airconditioned laboratory at the University of Stirling.

226 An individual flower, including the pedicel, was attached to the vibration transducer system
227 using the forceps. The forceps were used to hold the flower at the base of the five anthers (cf. De
228 Luca et al., 2013), and vibrations were thus directly transferred to the anthers in a similar manner as
229 when bees vibrate flowers. A single vibration (consisting of five 200 ms buzzes as described above),
230 was applied to the anthers of a flower, and the ejected pollen was collected in a 1.5 mL
231 microcentrifuge vial. Each flower was subjected to 30 consecutive vibrations for a grand total of 30 s
232 of buzzing time. Pollen was collected in separate vials for vibrations 1—10, 15, 20, 25, and 30. At the
233 end of the trial, we removed the anthers of the flower and placed them in a centrifuge tube with 200
234 µl of 70% ethanol. Each trial lasted 10-15 minutes. The remaining pollen in the flower was extracted
235 later with the help of a sonicating bath (D00351, Premier Farnell Ltd., Leeds, UK), which allowed us
236 to calculate the total amount of pollen grains in each flower we used in our pollen dispensing trials.

237 To estimate the number of pollen grains in each sample (including samples of the pollen
238 remaining in anthers), we used a particle counter (Multisizer 4e Coulter Counter, Indianapolis, USA).
239 Each pollen sample (suspended in 200 µl 70% ethanol) was added to 20 mL 0.9% NaCl solution. For
240 each sample, the amount of pollen was counted in two 1 mL subsamples. The pollen counts for
241 these subsamples were averaged and multiplied by 20 to obtain the total pollen count. For samples

242 with higher pollen concentrations, such as those containing the pollen remaining in the anther, we
243 added the pollen samples to 100 or 200 mL NaCl solution and multiplied the averaged pollen count
244 by 100 or 200 respectively to obtain the total pollen count. Blank samples, containing only 0.9% NaCl
245 solution were run at the beginning of a session and regularly between samples to ensure calibration
246 accuracy.

247 **Characterising pollen dispensing curves-**

248 To characterize the pollen dispensing curves, we fitted exponential decay curves for each flower
249 using the *nls* function in R ver. 3.6.0 (R Core Team, 2019). The decay curves followed the function:

$$250 \quad y = a * (1 - b)^x$$

251 where *y* represents the percentage of pollen released in a vibration, and *x* represents the vibration
252 number. The parameter *a* represents the intercept of the pollen dispensing curve, and the
253 parameter *b* represents the percentage decrease in the amount of pollen released in each successive
254 vibration (e.g., if *b* = 0.3, then 30% of the remaining pollen is released in each successive vibration).
255 Model parameters were estimated separately for each flower using the *nls* function. The percentage
256 pollen released per vibration was calculated by dividing the amount of pollen released per vibration
257 by the total amount of pollen in a flower.

258 **Measuring anther traits-**

259 For each flower used in our trials, we measured three traits for the pollinating and feeding anthers
260 separately, after pollen had been extracted. We measured: (1) the anther length, (2) the anther
261 breadth at base of the anther, and (3) the area of the pores (Appendix S4). Anther length and
262 breadth were measured using a dissection microscope and callipers. For each flower, all four feeding
263 anthers were measured, and lengths and breadths were averaged across the feeding anthers to
264 calculate a single value per flower. To calculate the anther pore area, we took SEM photographs of
265 one feeding and one pollinating anther per flower, and we measured the area of the pores from
266 photographs using ImageJ v1.52 (Schneider et al., 2012). Variation in traits between species can be
267 seen in Figs. 1 & 2.

268 **Variation in pollen dispensing curves across flower types-**

269 To assess whether pollen dispensing schedules vary between flower types, we subjected *Solanum*
270 *rostratum*, *S. fructu-tecto*, *S. grayi* var. *grandiflorum*, *S. grayi* var. *grayi*, *S. citrullifolium*, and *S.*
271 *heterodoxum* flowers to simulated vibration stimuli as described above. All vibration stimuli had a
272 peak velocity of 80 mm/s. We used this velocity as it corresponds to velocities which have been

273 recorded for bees on flowers (De Luca and Vallejo-Marín, 2013). Pollen dispensing curves were
274 characterized for ten flowers per species, except for *S. fructu-tecto* where only five flowers were
275 used.

276 To compare the pollen dispensing curves, we extracted two response variables from each
277 curve. Firstly, we extracted the amount of pollen released from the first simulated vibration, which
278 reflects the amount of pollen reward a pollinator will receive in a single visit. Secondly, we estimated
279 the rate of pollen release (i.e., the dispensing rate) as represented by b in the exponential decay
280 function. For example, if $b = 0.2$, then 20% of the remaining pollen in the anther is released in each
281 sequential vibration.

282 To compare pollen dispensing between small and large flower types, we analysed each of
283 the three phylogenetic pairs separately (series *Androceras*, *Pacificum* and *Violaceiflorum*). After
284 testing for normality, we used nonparametric Wilcoxon rank sum tests. We chose to perform three
285 separate within-clade tests, instead of a single parametric omnibus test across all species, because
286 both the non-normality of our data and our small sample sizes that would prevent fitting more
287 complex parametric models with clade * anther-type interactions. Importantly, our tests allow
288 assessing whether differences between small- and large-flowered species are clade specific. Because
289 we performed multiple tests, we used the Holm method to adjust p-values (similar to the Bonferroni
290 correction but with a lower risk of introducing type II error). In addition to releasing pollen across
291 multiple vibrations, plants can potentially further stagger pollen release across hours or days. We
292 tested for this by comparing the total percentage of pollen that was released from anthers across
293 the 30 vibrations between anther types within clades using Wilcoxon rank sum tests with Holm-
294 adjusted p-values.

295 ***Effect of vibration properties on pollen dispensing-***

296 We assessed the influence of vibration properties on pollen dispensing schedules by applying
297 simulated vibrations to flowers of two species: *Solanum citrullifolium* (large flower type) and *S.*
298 *heterodoxum* (small flower type). We focused on the effects of variation in velocity because previous
299 work has shown that velocity is positively associated with the amount of pollen released in a single
300 vibration (De Luca et al., 2013). We applied three peak velocity treatments: 80, 40, and 20 mm/s.
301 These values are within the range of previously recorded bee vibrations (De Luca et al., 2013).
302 Dispensing curves were characterized for nine to ten flowers for each treatment and species (Table
303 1). We used the same response variables as in the previous section (i.e., percentage of pollen
304 released in the first vibration and the dispensing rate), and we compared these response variables
305 across the three velocity treatments within each species separately using analysis of variance

306 (ANOVA) and Tukey posthoc tests. Further, we compared the total amount of pollen released per
307 treatment within each species using ANOVA and Tukey posthoc tests.

308 ***Association between pollen dispensing schedules and anther traits-***

309 If consistent differences are found between large- and small-flowered taxa, the question of what
310 causes those differences remains. One hypothesis is that the anther traits specified in the Buchmann
311 and Hurley (1978) model predicts the rate of pollen release. The anther traits Buchmann and Hurley
312 (1978) used in their model of pollen release from poricidal anthers include the area of the pore (A'),
313 the area of the anther locule along the wall perpendicular to the movement direction of the anther
314 (A), and the internal volume of the anther's locule (ϑ). Because of the complexity of anther shapes
315 and the technical difficulty of accurately estimating the internal dimensions of the anther locule, we
316 used external anther area (length x breadth of the anther; Buchmann and Hurley, 1978; Appendix
317 S4) as a proxy of locule area A . We kept the pollinating and feeding anther traits separately, rather
318 than combining their areas, because of the morphological differences between these anther types
319 which may have different effects on pollen release. Further, because flowers contain four feeding
320 anthers and one pollinating anther, we multiplied the values of both the pore area and the anther
321 wall area of the feeding anther by four to obtain total areas for each flower. Because kinetic energy
322 was kept constant in our pollen extraction trials, we could directly assess the association between
323 pollen dispensing schedules and anther traits.

324 To determine whether the amount of pollen released in the first vibration is related to
325 anther traits, we implemented a negative binomial mixed effect model (LMM) in *lme4* (Bates et al.,
326 2015). We used the amount of pollen released in the first vibration as response variable and the four
327 anther traits (i.e., pore area and anther wall area for pollinating and feeding anthers separately) as
328 predictor variables. Because the total amount of pollen grains varied between flowers, we also
329 included the total amount of pollen grains per flower as offset in the model. We added species
330 identity as a random effect. Similarly, we evaluated the association between pollen dispensing rate
331 and anther traits. Because the dispensing rate metric (b) is bounded between 0 and 1, we conducted
332 a logistic mixed effect model (GLMM) using the dispensing rate as the response variable and the four
333 anther traits as the predictor variables, with species identity as a random effect.

334

335 RESULTS

336 ***Pollen dispensing-***

337 Plant species varied in the amount of pollen grains that were present in flowers, with *Solanum*
338 *heterodoxum* containing the fewest pollen grains ($22 \times 10^3 \pm 8 \times 10^3$; median \pm se) and *S. grayi* var.
339 *grandiflorum* containing the most ($446 \times 10^3 \pm 17 \times 10^3$; Table 1). Small-flowered taxa consistently
340 contained fewer pollen grains than their large-flowered counterparts (Table 1). The amount of
341 pollen released decreased gradually with an increasing number of vibrations applied, and no pollen
342 was released by the 30th vibration (Fig. 3), despite large amounts of pollen remaining in the anthers
343 (Fig. 4c). The pollen dispensing curves thus showed exponential decay, with most pollen released in
344 the first vibration (Fig. 3).

345 ***Variation in pollen dispensing schedules between flower types-***

346 The percentage of pollen released in the first vibration varied between flower types, and for all three
347 phylogenetic clades, more pollen was released in the first vibration for small flower types than large
348 flower types (SC-SH: $W = 8$, $p < 0.001$, $p_{\text{adjusted}} = 0.002$; SR-SF: $W = 1$, $p = 0.001$, $p_{\text{adjusted}} = 0.003$; SGN-
349 SGG: $W = 18$, $p = 0.01$, $p_{\text{adjusted}} = 0.01$; Table 1; Figs. 3 & 4). Across our six taxa, *Solanum heterodoxum*
350 released the largest percentage of pollen grains in the first vibration ($46.03\% \pm 5.88$; median \pm se)
351 and *S. grayi* var. *grandiflorum* released the smallest ($0.58\% \pm 0.13$; Table 1). For most species, the
352 amount of pollen released in the first vibration represented more than half of the pollen that was
353 released during the 30 vibrations (Table 2).

354 For two of the three clades, the dispensing rates were higher in small-flowered taxa than
355 large-flowered taxa, indicating differences in the shapes of the curves. Specifically, the dispensing
356 rates for small-flowered taxa were higher than those of large flower types for the SR-SF clade ($W = 3$,
357 $p = 0.005$, $p_{\text{adjusted}} = 0.01$) and marginally significant for the SC-SH clade ($W = 24$, $p = 0.05$, $p_{\text{adjusted}} =$
358 0.10), but not for the SGN-SGG clade ($W = 48$, $p = 0.91$, $p_{\text{adjusted}} = 0.91$; Figs. 3 & 4; Table 2). The fast
359 dispensing rates in small-flowered taxa show that these taxa required fewer vibrations to release all
360 the available pollen than large-flowered taxa.

361 None of the six taxa released all their pollen during 30 vibrations, despite no pollen being
362 released after 30 vibrations. The total amount of pollen released varied strongly between the
363 species of each phylogenetically independent contrast, with large-flowered taxa releasing
364 proportionally fewer pollen grains in 30 vibrations than their small-flowered sister taxon (SC-SH: $W =$
365 2 , $p < 0.001$, $p_{\text{adjusted}} < 0.001$; SR-SF: $W = 48$, $p = 0.002$, $p_{\text{adjusted}} = 0.005$; SGN-SGG: $W = 88$, $p = 0.002$,
366 $p_{\text{adjusted}} = 0.005$; Fig. 4; Table 1). We also observed differences between clades, where the largest
367 proportion of pollen was released by the SC-SH clade and the smallest proportion was released by
368 the SGG-SGN clade.

369 ***Effect of vibration properties on pollen dispensing schedules-***

370 The application of different peak vibration velocities resulted in different pollen dispensing
371 schedules. Generally, lower vibration velocities resulted in slower pollen release and less total pollen
372 released over 30 vibrations.

373 We tested whether the percentage of pollen released in the first vibration varied with
374 vibration velocity, and we found effects of vibration velocity for both the large-flowered *S.*
375 *citrullifolium* ($F_{2,27} = 11.44$, $p < 0.001$) and the small-flowered *S. heterodoxum* ($F_{2,25} = 21.86$, $p < 0.001$)
376 (Figs. 5 & 6). Tukey posthoc tests showed that for *S. citrullifolium*, a velocity of 80 mm/s released
377 more pollen in the first vibration than both lower velocity vibrations ($SC_{40\text{mm/s}}$: $p = 0.002$; $SC_{20\text{mm/s}}$: $p <$
378 0.001). For each sequential lower velocity vibration, we observed a more than four times decrease in
379 the percentage pollen released (Table 1). Similarly, a velocity of 80 mm/s released more pollen in *S.*
380 *heterodoxum* plants than both lower velocity vibrations ($SH_{40\text{mm/s}}$: $p < 0.001$; $SH_{20\text{mm/s}}$: $p < 0.001$), and
381 we observed a nine-fold decrease in percentage pollen release between velocities of 80 mm/s and
382 40 mm/s. No differences in pollen released in the first vibration were present between velocities of
383 40 mm/s and 20 mm/s for either species (SC : $p = 0.85$; SH : $p = 0.76$).

384 Further, we found differences in the pollen dispensing rates when different vibration
385 velocities were applied. These differences were observed both in *S. citrullifolium* ($F_{2,27} = 10.64$, $p <$
386 0.001) and in *S. heterodoxum* ($F_{2,25} = 11.50$, $p < 0.001$) (Fig. 6). For *S. citrullifolium*, a velocity of 80
387 mm/s released pollen quicker than velocities of 40 mm/s ($p = 0.001$) and 20 mm/s ($p < 0.001$), which
388 shows that more vibrations are required to release the available pollen grains when vibration
389 velocities are lower. We observed a three-fold decrease in dispensing rate with a decrease in
390 vibration velocity. Similarly, a velocity of 80 mm/s released pollen quicker in *S. heterodoxum* than
391 velocities of 40 mm/s ($p = 0.02$) and 20 mm/s ($p < 0.001$). However, no differences in pollen
392 dispensing rates were detected between velocities of 40 mm/s and 20 mm/s (SC : $p = 0.91$; SH : $p =$
393 0.45).

394 In addition to changes in the shape of the pollen dispensing curves, differences in vibration
395 velocity also influenced the total amount of pollen grains that were ejected, both for *S. citrullifolium*
396 ($F_{2,27} = 4.906$, $p = 0.01$, Figs. 5 & 6) and for *S. heterodoxum* ($F_{2,25} = 25.67$, $p < 0.001$, Figs. 5 & 6). For *S.*
397 *citrullifolium*, Tukey posthoc tests showed a significant decrease in the total amount of pollen
398 released between 80 and 20 mm/s ($p = 0.01$), but not between 80 and 40 mm/s ($p = 0.26$) nor
399 between 40 and 20 mm/s ($p = 0.28$). Similarly, Tukey posthoc tests showed a significant decrease in
400 the total amount of pollen released for *S. heterodoxum* between 80 and 40 mm/s ($p < 0.001$) and
401 between 80 and 20 mm/s ($p < 0.001$), but not between 40 and 20 mm/s ($p = 0.41$).

402 ***Association between pollen dispensing schedules and anther traits-***

403 We tested whether anther traits (i.e., anther wall area and anther pore size) of the feeding and
404 pollinating anthers relate to pollen dispensing, as hypothesized by Buchmann and Hurley (1978). The
405 amount of pollen released in the first vibration was negatively associated with the pollinating anther
406 wall area ($z = -2.232$, $p = 0.03$, Table 2), showing that flowers with larger pollinating anthers release
407 less pollen in the first vibration than those with smaller pollinating anthers. Thus, for each 1 mm^2
408 increase in pollinating anther area, the log count of pollen released in the first vibration decreases by
409 0.075 (= 7.8% decrease in pollen grains released). Similarly, pollen dispensing rates were negatively
410 associated with the pollinating anther wall area ($z = -1.952$, $p = 0.05$, Table 2), showing that flowers
411 with larger pollinating anthers release pollen more slowly than flowers with smaller anthers. Thus,
412 with each 1 mm^2 increase in pollinating anther area, the dispensing rate was 10.2% lower. We found
413 no effect of anther pore size in either analysis (Table 2).

414

415 **DISCUSSION**

416 Our study is the first to systematically investigate the effects of anther morphology and vibration
417 properties on pollen dispensing schedules in buzz-pollinated plants. When applying bee-like
418 vibrations directly to anthers, we found consistent differences in pollen release rates between
419 anther types, where the large anther type released pollen more gradually than the small anther
420 type. Higher vibration velocities resulted in more pollen released in the first vibration and faster
421 pollen release rates, irrespective of the anther type. We thus show that both anther morphology and
422 bee vibrations are associated with pollen release schedules, and likely pollen export, in buzz-
423 pollinated plants. Additionally, we found that larger pollinating anther areas were associated with
424 less pollen released in the first vibration and a slower dispensing rate, showing the potential for
425 relating individual anther traits to pollen release in poricidal taxa.

426 ***Pollen dispensing schedules in buzz-pollinated taxa-***

427 Many plant species stagger the pollen release of individual flowers across hours or days (Buchmann
428 et al., 1977; Harder and Barclay, 1994; Sargent, 2003; Castellanos et al., 2006b; Li et al., 2014;
429 Dellinger, Pöllabauer, et al., 2019), and here we show that flowers can also limit pollen release
430 across shorter timeframes (i.e., seconds and minutes). For all six taxa, pollen was released across
431 multiple vibrations, with a smaller amount of pollen released in each successive vibration. This
432 suggests that multiple visits or extended visits by vibrating pollinators are required to extract all of
433 the pollen available for release (see Larson and Barrett, 1999), and that bees would receive the

434 largest pollen rewards in the first vibration. Most flowers required between three and ten vibrations
435 to release all available pollen grains, which translates to 6 to 20 seconds of buzzing. Our results align
436 with the field observations made by Bowers (1975) which showed that bees tend to spend more
437 time (i.e., 3 – 15 seconds) on newly opened *S. rostratum* flowers and less time on previously visited
438 flowers, presumably matching their visitation lengths with pollen availability.

439 In line with work on non-poricidal taxa, we also found that pollen release is staggered over
440 longer timeframes. Four of our six taxa released only a small percentage of their total pollen across
441 the thirty vibrations we applied (<20%, median, Fig. 3), even though no pollen was released during
442 the last few vibrations of each trial (see Fig. 2). Because this secondary pollen dosing mechanism
443 does not seem to result from anther morphology, it is likely that pollen maturation or drying of
444 pollenkitt is staggered in these plants, as is seen in other buzz-pollinated taxa (Buchmann et al.,
445 1977; Corbet et al., 1988; King and Ferguson, 1994; King and Buchmann, 1996). Staggering pollen
446 maturation can also allow dynamic adjustment of pollen release schedules to pollinator visitation
447 rates. For instance, if a flower that staggers pollen maturation receives its first visit on the second
448 day of anthesis (e.g., under low visitation rates), then a larger quantity of pollen will be available for
449 extraction than a flower which is visited on the first day (Harder and Barclay 1994). This dynamic
450 adjustment of pollen release to pollinator visitation rates is predicted by theoretical models (Harder
451 and Wilson 1994) and has been shown to occur in other poricidal taxa (Harder and Barclay, 1994;
452 Dellinger, Pöllabauer, et al., 2019).

453 ***Shifts in pollen dispensing schedules between flower types-***

454 Theoretical models predict that pollen release schedules should be optimized to pollinator grooming
455 behaviour and pollinator visitation rates (Harder and Thomson, 1989; Harder and Wilson, 1994;
456 LeBuhn and Holsinger, 1998), and empirical work has shown support for these models (Sargent,
457 2003; Castellanos et al., 2006; Li et al., 2014). A notable study by Castellanos et al. (2006) showed
458 that parallel shifts in *Penstemon* between bee and hummingbird pollination are associated with
459 shifts in anther morphology and pollen dispensing schedules. Similarly, we show that closely-related
460 species in *Solanum* sect. *Androceras*, that have undergone parallel shifts in anther morphology
461 (Vallejo-Marín et al., 2014), have also undergone parallel shifts in their pollen dispensing schedules.

462 There are at least three non-mutually exclusive hypotheses that could explain the *transition*
463 in dispensing strategy we observed here from slow dispensing in large-flowered taxa to quicker
464 dispensing in small-flowered species: (i) adaptation to a shift in higher selfing rates, (ii) adaptation to
465 a shift in pollinator environment (i.e., lower visitation rate and higher pollen transfer efficiency), and
466 (iii) non-adaptive by-product of the evolution of smaller anthers, which we discuss in turn. (i) *Shift to*

467 *selfing in small flowers*. The rapid release of pollen in highly selfing taxa would be expected in small-
468 flowered taxa if selfing is facilitated by pollinators, and thus a single visit by a buzz-pollinating bee
469 can maximise fitness. Moreover, higher rates of pollen release may also be favourable with
470 autonomous selfing if other sources of disturbance to flowers (e.g., induced by wind or non-buzzing
471 floral visitors) might allow pollen release without the assistance of vibrating bees. Although previous
472 work shows that the small-flowered taxa in *Solanum* sect. *Androceras* exhibit traits that correspond
473 to a self-pollination syndrome (Vallejo-Marín et al., 2014; Rubini-Pisano et al., in prep), we currently
474 lack field-estimates of selfing rates of the small-flowered species. Hence this hypothesis remains to
475 be tested further. (ii) *Shift to pollination environments with lower visitation and/or higher pollen*
476 *transfer efficiency*. In principle, if small-flowered taxa are visited less frequently or visited by
477 pollinators that groom less and efficiently transfer pollen to conspecifics, quicker dispensing
478 strategies could be adaptive. Apart from *S. rostratum*, little is known about the pollination ecology of
479 Section *Androceras*. Whalen (1978) suggested that the transition to small flowers in *Solanum grayii*
480 var. *grayii* was associated with a shift to visitation by smaller bees compared to the large-flowered *S.*
481 *grayii* var. *grandiflorum*, but we do not know of any detailed characterisations of their pollination
482 ecology. In the large-flowered species *S. rostratum*, both large (e.g. *Xylocopa*) and small bees (e.g.,
483 *Lasioglossum*) visit their flowers (Solis-Montero et al. 2015), although larger bees are more likely to
484 contact the sexual organs during visitation (Solis-Montero and Vallejo-Marín 2017). In general, it is
485 unknown to what extent pollinators sort themselves by size across these plant species, and whether
486 visitation rate or pollen-grooming efficiency consistently varies with bee size. Testing the hypothesis
487 that the shift in pollen dispensing is associated with changes in pollination environment (whether
488 associated with smaller pollinators or not) requires additional field observations, particularly among
489 the small-flowered species. (iii) *Non-adaptive by-product of the evolution of smaller flowers*. Changes
490 in dispensing rates in small-flowered taxa could result in the absence of selection on pollen
491 dispensing schedules. We found that smaller anther wall areas are associated with faster dispensing
492 rates. If selection favours the evolution of small flowers for any reason, then smaller flowers could
493 indirectly result in higher pollen dispensing rates simply due to a correlated reduction in anther size.
494 Although we show that pollen dispensing schedules vary consistently between these flower types,
495 field observations and experiments are required to determine the extent to which these three
496 hypotheses could explain differences in pollen dispensing schedules in these species.

497 ***The influence of vibration velocity on pollen dispensing schedules-***

498 For a variety of buzz-pollinated taxa, the amount of pollen released in a single vibration increases
499 with vibration velocity when artificial vibrations are applied (Harder and Barclay, 1994; King and
500 Buchmann, 1996; De Luca et al. 2013) as predicted by Buchmann and Hurley's (1978) model. Here,

501 we show for the first time that vibration velocity also influences the amount of pollen released in
502 successive vibrations. Low velocity vibrations resulted in slower pollen dispensing rates, with less
503 pollen dispensed during 30 vibrations. Accordingly, bees that produce low velocity vibrations are
504 unlikely to extract large pollen quantities. These bees would either need to visit multiple flowers or
505 they would potentially be discouraged from visiting these plants (Harder, 1990b; Nicholls and
506 Hempel de Ibarra, 2017). Poricidal anthers could thus act as filter to insect taxa that cannot produce
507 the necessary vibrations (De Luca and Vallejo-Marín, 2013; Sun and Rychtář, 2015; van der Kooi et
508 al., in press), and restrict access to pollen rewards in a similar way in which long nectar tubes exclude
509 insects with short proboscides from accessing nectar rewards (Newman et al., 2014; Santamaría and
510 Rodríguez-Gironés, 2015; Zung et al., 2015). This vibration filter might be particularly effective in
511 discouraging visitation from small bees that produce lower velocity vibrations (De Luca et al., 2013,
512 2019) and do not make contact with reproductive organs (Solís-Montero and Vallejo-Marín, 2017).
513 However, some bee taxa might be able to adjust their vibration velocities or duration (Harder and
514 Barclay, 1994; Morgan et al., 2016; Russell et al., 2016), resulting in increased pollen extraction at a
515 higher energy cost to the insect. Field observations of the large flowered *S. rostratum* have shown
516 that small buzzing bees frequently visit flowers (Solís-Montero et al., 2015), but larger taxa that
517 produce higher velocity vibrations (De Luca et al., 2019), such as *Bombus* and *Xylocopa*, are common
518 visitors (Whalen, 1978), as well as efficient pollinators (Solís-Montero and Vallejo-Marín, 2017).

519 Although bees that produce high velocity vibrations are the most effective at extracting
520 pollen, attracting such visitors might not always be the best strategy for plants. Optimal dispensing
521 schedules are contingent on pollinator grooming behaviours (Harder and Thomson, 1989), and if
522 bees groom large amounts of pollen per visit, then slower dispensing (as induced by lower velocity
523 vibrations) should theoretically result in higher plant fitness. Additionally, optimal dispensing
524 schedules are dependent on pollinator visitation rates, and these are likely to be dependent on bee
525 and plant community composition. Sargent (2003) showed that temporal changes in pollinator
526 community composition and visitation rates were associated with temporal within-species changes
527 in pollen dispensing rates. Thus, if pollinator visitation rates are low, quick dispensing will be
528 favoured, even if bees collect large amounts of pollen per visit. Optimal dispensing schedules are
529 thus expected to be adapted to the ecological community context, as well as the behaviour of bees.

530 ***Anther traits and pollen dispensing schedules-***

531 Our results clearly show that pollen dispensing schedules are associated with both anther type and
532 vibration properties. However, connecting pollen release schedule variation to specific anther traits
533 is much more challenging. We find that larger anther areas are associated with less pollen released

534 in the first vibration (Table 2a) and reduced pollen release rates (Table 2b). These effects are
535 statistically significant for pollinating anthers, but not for feeding anthers (Table 2). This suggests
536 that other aspects of the morphology and material properties of anthers that are not captured by
537 the model, such as anther tapering, anther inner surface structure or pollen properties, might be
538 important in pollen release. It further suggests that the ability of the current biophysical model to
539 predict pollen release might be more accurate for some anther morphologies than others, and this
540 warrants further investigation.

541 Our results contrast with the expectation generated by the Buchmann and Hurley (1978)
542 model that large anther locule areas should be associated with higher dispensing rates. However,
543 their model also predicts a negative association between anther locule volume and pollen dispensing
544 rates. Because anther wall area and anther locule volume are linked, we are potentially detecting
545 the effects of locule volume rather than locule wall area. Quantifying the internal volume of anther
546 locules is difficult but possible using techniques such as X-ray micro-computer tomography scanning
547 (Dellinger, Artuso, et al., 2019), and our work suggests that this is likely an important variable to
548 measure. The lack of a statistically significant association between pore size and pollen release
549 parameters is intriguing, but perhaps not unexpected given smaller variation in pore sizes than
550 anther areas (see Fig. 1), as well as the conflicting effects of pore area on pollen release in the
551 theoretical model of Buchmann and Hurley (1978).

552 CONCLUSIONS AND FUTURE DIRECTIONS

553 Our focal taxa stagger pollen release across multiple vibrations, and this is likely common in other
554 poricidal species (Corbet et al., 1988; Harder, 1990; Harder and Barclay, 1994; Dellinger, Pöllabauer,
555 et al., 2019). This gradual release of pollen will influence pollen export dynamics of plants and the
556 amount of reward that bees receive per visit. We show that high-velocity vibrations result in more
557 pollen released per vibration, and thus bees that can produce such vibrations will receive higher
558 reward quantities. The observed pollen dispensing schedules likely reflect an optimization that
559 maximises pollen export whilst providing sufficient rewards to pollinators.

560 Our results highlight the need for more empirical studies of pollen dispensing schedules in
561 buzz-pollinated plants, as well as for developing biophysical models of buzz-pollination that
562 incorporate additional aspects of the morphology, geometry and material properties of flowers. The
563 vibrations that the anthers experience depend both on the characteristics of bee vibrations (Switzer
564 et al., 2019; Pritchard and Vallejo-Marín, 2020) and on the properties of the floral structures
565 (Arroyo-Correa et al., 2019). For example, the transmission of vibrations through the flower can alter
566 the vibration that the anther experiences, e.g., by dampening the vibration velocity (King, 1993,

567 which can vary between closely-related taxa (Arroyo-Correa et al., 2019). In contrast, if the bee
568 vibrates the anther at its natural frequency (Nunes et al., 2020), resonance could amplify anther
569 velocity and result in higher pollen removal (King and Buchmann, 1996). Joint modelling and
570 experimental approaches to buzz pollination have the potential to help us understand the
571 biomechanics and function of a fascinating biological interaction involving thousands of plant and
572 bee species.

573

574 ACKNOWLEDGMENTS

575 We thank the members of the Vallejo-Marín lab for fruitful conversations on buzz-pollination and
576 help with plant maintenance, with particular thanks to Carlos Pereira Nunes. We thank Ian
577 Washbourne and George MacLeod for assistance with the use of the particle counter and SEM
578 respectively, and Boris Igic and Lislie Solís-Montero for collaborating with the fieldwork to collect
579 seed material. We thank the Associate Editor and two anonymous reviewers for their constructive
580 comments. The project was made possible by the Royal Society of London and the Newton Fund
581 through a Newton International Fellowship to JEK (NIF/R1/181685), by a Scottish Plant Health
582 License (PH/38/2018-2020), and a research grant from The Leverhulme Trust (RPG-2018-235) to
583 MVM.

584

585 AUTHOR CONTRIBUTIONS

586 Investigation (conducting experiments and data collection): JEK. Conceptualisation, visualisation,
587 formal analysis, writing and funding acquisition: JEK and MVM.

588

589 DATA AVAILABILITY

590 The data associated with this paper is available at the University of Stirling's DataSTORRE repository.

591

592 SUPPORTING INFORMATION

593 Additional Supporting Information may be found online in the supporting information section at the
594 end of the article.

595 Appendix S1. Plant material of *Solanum* section *Androceras* used in this study.

596 Appendix S2. Artificial vibrations applied to anthers. (a) Each stimulus consisted of five short
597 vibration pulses of 0.2 s long, with 0.2 s of silence between pulses. (b) The beginning of each 0.2 s
598 pulse consisted of a short fade-in, which is similar to what bees produce and it ensures that the
599 wave is transmitted in the expected manner.

600 Appendix S3. The custom-made vibration transducer system. Vibrations were transferred from a
601 laptop to (1) a speaker. From there, vibrations were transferred to (2) a metal rod that was attached
602 in the speaker with glue. Vibrations then travelled from the rod through (3) a metal clip that was
603 tightly attached to the metal rod and fixed using glue. From there, vibrations were transferred to (4)
604 forceps, and then to (5) anthers. The anthers were clasped approximately where a bee would attach.
605 Please note that in our experiments, we used storkbill short blunt forceps (D4045, Watkins &
606 Doncaster, UK) and not the long-pronged forceps depicted here.

607 Appendix S4. For each anther, the length (solid line) and breadth (dashed line) was measured. For
608 each anther type within a flower the pore area was measure for one feeding and one pollinating
609 anther. The photo shows a SEM image of a *Solanum fructu-tecto* feeding anther. The scale bar
610 represents 200 μm .

611

612 LITERATURE CITED

- 613 Arceo-Gómez, G., M. L. Martínez, V. Parra-Tabla, and J. G. García-Franco. 2011. Anther and stigma
614 morphology in mirror-image flowers of *Chamaecrista chamaecristoides* (Fabaceae):
615 Implications for buzz pollination. *Plant Biology* 13: 19–24.
- 616 Arroyo-Correa, B., C. Beattie, and M. Vallejo-Marín. 2019. Bee and floral traits affect the
617 characteristics of the vibrations experienced by flowers during buzz pollination. *Journal of*
618 *Experimental Biology* 222: jeb198176.
- 619 Bowers, K.A.W. 1975. The pollination ecology of *Solanum rostratum* (Solanaceae). *American Journal*
620 *of Botany* 62: 633–638.
- 621 Buchmann, S. L., C. E. Jones, and L.J. Colin. 1977. Vibratile pollination of *Solanum douglasii* and *S.*
622 *xanti* (Solanaceae) in southern California. *The Wasmann Journal of Biology* 35: 1–25.
- 623 Buchmann, S. L. 1983. Buzz pollination in angiosperms. *Handbook of Experimental Pollination*
624 *Biology*. In: Jones CE, Little RJ, eds. *Handbook of experimental pollination biology*. New York,
625 NY: Scientific and Academic Editions, 73–113.
- 626 Buchmann, S. L., and J. P. Hurley. 1978. A biophysical model for buzz pollination in angiosperms.
627 *Journal of Theoretical Biology* 72: 639–657.
- 628 Cardinal, S., S. L. Buchmann, and A. L. Russell. 2018. The evolution of floral sonication: a pollen
629 foraging behavior used by bees (Anthophila). 590–600.
- 630 Castellanos, M. C., P. Wilson, S. J. Keller, A. D. Wolfe, and J. D. Thomson. 2006. Anther evolution:
631 pollen presentation strategies when pollinators differ. *The American Naturalist* 167: 288–296.
- 632 Corbet, S. A., H. Chapman, and N. Saville. 1988. Vibratory pollen collection and flower form: bumble-
633 bees on *Actinidia*, *Symphytum*, *Borago* and *Polygonatum*. *Functional Ecology* 2: 147-155.
- 634 Corbet, S. A., and S. Q. Huang. 2014. Buzz pollination in eight bumblebee-pollinated *Pedicularis*
635 species: Does it involve vibration-induced triboelectric charging of pollen grains? *Annals of*
636 *Botany* 114: 1665–1674.
- 637 Dellinger, A. S., S. Artuso, S. Pamperl, F. A. Michelangeli, D. S. Penneys, D. M. Fernández-Fernández,
638 M. Alvear, et al. 2019. Modularity increases rate of floral evolution and adaptive success for
639 functionally specialized pollination systems. *Communications Biology* 2: 453.
- 640 Dellinger, A. S., M. Chartier, D. Fernández-Fernández, D. S. Penneys, M. Alvear, F. Almeda, F. A.
641 Michelangeli, et al. 2019. Beyond buzz-pollination—departures from an adaptive plateau lead to

642 new pollination syndromes. *New Phytologist* 221: 1136–1149.

643 Dellinger, A. S., L. Pöllabauer, M. Loreti, J. Czurda, and J. Schönenberger. 2019. Testing functional
644 hypotheses on poricidal anther dehiscence and heteranthery in buzz-pollinated flowers. *Acta*
645 *ZooBot Austria* 156: 197–214.

646 Dulberger, R., M. B. Smith, and K. S. Bawa. 1994. The stigmatic orifice in *Cassia*, *Senna*, and
647 *Chamaecrista* (Caesalpinaceae): Morphological variation, function during pollination, and
648 possible adaptive significance. *American Journal of Botany* 81: 1390–1396.

649 Faegri, K. 1986. The solanoid flower. *Transactions of the Botanical Society of Edinburgh* 45: 51–59.

650 Harder, L. D. 1990. Behavioral responses by bumble bees to variation in pollen availability. *Oecologia*
651 85: 41–47.

652 Harder, L. D., and R. M. R. Barclay. 1994. The functional significance of poricidal anthers and buzz
653 pollination: controlled pollen removal from *Dodecatheon*. *Functional Ecology* 8: 509–517.

654 Harder, L. D., and S. D. Johnson. 2009. Darwin's beautiful contrivances: evolutionary and functional
655 evidence. *New Phytologist* 183: 530–545.

656 Harder, L. D., and J. D. Thomson. 1989. Evolutionary options for maximizing pollen dispersal of
657 animal-pollinated plants. *The American Naturalist* 133: 323–344.

658 Harder, L. D., and W. G. Wilson. 1994. Floral evolution and male reproductive success: Optimal
659 dispensing schedules for pollen dispersal by animal-pollinated plants. *Evolutionary Ecology* 8:
660 542–559.

661 Harris, J. A. 1905. The dehiscence of anthers by apical pores. *Missouri Botanical Garden Report*: 167–
662 257.

663 Holsinger, K. E., and J. D. Thomson. 1994. Pollen discounting in *Erythronium grandiflorum*: mass-
664 action estimates from pollen transfer dynamics. *The American Naturalist* 144: 799–812.

665 King, M. J. 1993. Buzz foraging mechanism of bumble bees. *Journal of Apicultural Research* 32: 41–
666 49.

667 King, M. J., and S. L. Buchmann. 2003. Floral sonication by bees: Mesosomal vibration by *Bombus*
668 and *Xylocopa*, but not *Apis* (Hymenoptera: Apidae), ejects pollen from poricidal anthers.
669 *Journal of Kansas Entomological Society* 76: 295–305.

670 King, M. J., and S. L. Buchmann. 1996. Sonication dispensing of pollen from *Solanum laciniatum*

671 flowers. *Functional Ecology* 10: 449–456.

672 King, M. J., S. L. Buchmann, and H. Spangler. 1996. Activity of asynchronous flight muscle from two
673 bee families during sonication (buzzing). *Journal of Experimental Biology* 199: 2317–2321.

674 King, M. J., and A. M. Ferguson. 1994. Vibratory Collection of *Actinidia deliciosa* (Kiwifruit) Pollen.
675 *Annals of Botany* 74: 479–482.

676 Knapp, S. 2002. Floral diversity and evolution in the Solanaceae. In: Developmental genetics and
677 plant evolution, 267–297.

678 Larson, B. M. H., and S. C. H. Barrett. 1999. The pollination ecology of buzz-pollinated *Rhexia*
679 *virginica* (Melastomataceae). *American Journal of Botany* 86: 502–511.

680 LeBuhn, G., and K. Holsinger. 1998. A sensitivity analysis of pollen-dispensing schedules. *Evolutionary*
681 *Ecology* 12: 111–121.

682 Li, X. X., H. Wang, R. W. Gituru, Y. H. Guo, and C. F. Yang. 2014. Pollen packaging and dispensing:
683 Adaption of patterns of anther dehiscence and flowering traits to pollination in three
684 *Epimedium* species. *Plant Biology* 16: 227–233.

685 De Luca, P. A., S. Buchmann, C. Galen, A. C. Mason, and M. Vallejo-Marín. 2019. Does body size
686 predict the buzz-pollination frequencies used by bees? *Ecology and Evolution* 9: 4875–4887.

687 De Luca, P. A., L. F. Bussière, D. Souto-Vilaros, D. Goulson, A. C. Mason, and M. Vallejo-Marín. 2013.
688 Variability in bumblebee pollination buzzes affects the quantity of pollen released from
689 flowers. *Oecologia* 172: 805–816.

690 De Luca, P. A., and M. Vallejo-Marín. 2013. What’s the ‘buzz’ about? The ecology and evolutionary
691 significance of buzz-pollination. *Current Opinion in Plant Biology* 16: 429–435.

692 Minnaar, C., B. Anderson, M. L. De Jager, and J. D. Karron. 2019. Plant–pollinator interactions along
693 the pathway to paternity. *Annals of Botany* 123: 225–245.

694 Morgan, T., P. Whitehorn, G. C. Lye, and M. Vallejo-Marín. 2016. Floral sonication is an innate
695 behaviour in bumblebees that can be fine-tuned with experience in manipulating flowers.
696 *Journal of Insect Behavior* 29: 233–241.

697 Newman, E., J. Manning, and B. Anderson. 2014. Matching floral and pollinator traits through guild
698 convergence and pollinator ecotype formation. *Annals of Botany* 113: 373–384.

699 Nicholls, E., and N. Hempel de Ibarra. 2017. Assessment of pollen rewards by foraging bees.

700 *Functional Ecology* 31: 76–87.

701 Nunes, C.E.P., L. Nevard, F. Montealegre-Zapata, and M. Vallejo-Marin. 2020. Are flowers tuned to
702 buzzing pollinators? Variation in the natural frequency of stamens with different morphologies
703 and its relationship to bee vibrations. *bioRxiv*. doi: <https://doi.org/10.1101/2020.05.19.104422>.

704 Ollerton, J., R. Winfree, and S. Tarrant. 2011. How many flowering plants are pollinated by animals?
705 *Oikos* 120: 321–326.

706 Pritchard, D.J., and M. Vallejo-Marín. 2020. Floral vibrations by buzz-pollinating bees achieve higher
707 frequency , velocity and acceleration than flight and defence vibrations. *Journal of*
708 *Experimental Biology* 223:11.

709 R Core Team. 2019. R: A language and environment for statistical computing. R Core Team. Vienna,
710 Austria. <http://www.R-project.org/>

711 Rosi-Denadai, C. A., P. C. S. Araújo, L. A. de O. Campos, L. Cosme, and R. N. C. Guedes. 2018. Buzz-
712 pollination in Neotropical bees: genus-dependent frequencies and lack of optimal frequency for
713 pollen release. *Insect Science* 27: 133–142.

714 Rubini Pisano, A., M. Vallejo-Marín, S. Benitez-Vieyra, and J. Fornoni. In review. From large to small
715 flowers in Solanum (Section Androceras): a multivariate perspective.

716 Russell, A. L., A. S. Leonard, H. D. Gillette, and D. R. Papaj. 2016. Concealed floral rewards and the
717 role of experience in floral sonication by bees. *Animal Behaviour* 120: 83–91.

718 Santamaría, L., and M. a. Rodríguez-Gironés. 2015. Are flowers red in teeth and claw? Exploitation
719 barriers and the antagonist nature of mutualisms. *Evolutionary Ecology* 29: 311–322.

720 Sargent, R. D. 2003. Seasonal changes in pollen-packaging schedules in the protandrous plant
721 Chamerion angustifolium. *Population Ecology* 135: 221–226.

722 Särkinen, T., L. Bohs, R. G. Olmstead, and S. Knapp. 2013. A phylogenetic framework for evolutionary
723 study of the nightshades (Solanaceae): A dated 1000-tip tree. *BMC Evolutionary Biology* 13.

724 Schlindwein, C., D. Wittmann, C. F. Martins, a. Hamm, J. a. Siqueira, D. Schiffler, and I. C. MacHado.
725 2005. Pollination of *Campanula rapunculus* L. (Campanulaceae): How much pollen flows into
726 pollination and into reproduction of oligolectic pollinators? *Plant Systematics and Evolution*
727 250: 147–156.

728 Schneider, C. A., W. S. Rasband, and K. W. Eliceiri. 2012. NIH Image to ImageJ: 25 years of image
729 analysis. *Nature Methods* 9: 671–675.

- 730 Solis-Montero, L., C. Vergara, and M. Vallejo-Marín. 2015. High incidence of pollen theft in natural
731 populations of a buzz-pollinated plant. *Arthropod-Plant Interactions* 9: 599-611.
- 732 Solis-Montero, L., and M. Vallejo-Marín. 2017. Does the morphological fit between flowers and
733 pollinators affect pollen deposition? An experimental test in a buzz-pollinated species with
734 anther dimorphism. *Ecology and Evolution* 7: 2706-2715.
- 735 Stern, S. R., T. Weese, and L. A. Bohs. 2010. Phylogenetic relationships in *Solanum* section
736 *Androceras* (Solanaceae). *Systematic Botany* 35: 885–893.
- 737 Sun, S., and J. Rychtář. 2015. The screening game in plant–pollinator interactions. *Evolutionary*
738 *Ecology* 29: 479–487.
- 739 Switzer, C. M., and S. A. Combes. 2017. Bumblebee sonication behavior changes with plant species
740 and environmental conditions. *Apidologie* 48: 223–233.
- 741 Switzer, C.M., A. Russell, D. Papaj, S. Combes, and R. Hopkins. 2019. Sonicating bees demonstrate
742 flexible pollen extraction without instrumental learning. *Current Zoology* 65: 425-436.
- 743 Thomson, J. D. 1986. Pollen transport and deposition by bumble bees in *Erythronium*: influences of
744 floral nectar and bee grooming. *Journal of Ecology* 74: 329–341.
- 745 Vallejo-Marín, M. 2019. Buzz pollination: studying bee vibrations on flowers. *New Phytologist* 224:
746 1068–1074.
- 747 Vallejo-Marín, M., J. S. Manson, J. D. Thomson, and S. C. H. Barrett. 2009. Division of labour within
748 flowers: Heteranthery, a floral strategy to reconcile contrasting pollen fates. *Journal of*
749 *Evolutionary Biology* 22: 828–839.
- 750 Vallejo-Marín, M., E. M. Da Silva, R. D. Sargent, and S. C. H. Barrett. 2010. Trait correlates and
751 functional significance in flowering of heteranthery plants. *New Phytologist* 188(2): 418-425.
- 752 Vallejo-Marín, M., C. Walker, P. Friston-Reilly, L. Solís-Montero, and B. Igic. 2014. Recurrent
753 modification of floral morphology in heterantherous *Solanum* reveals a parallel shift in
754 reproductive strategy. *Philosophical Transactions of the Royal Society B: Biological Sciences*
755 369: 20130256.
- 756 van der Kooij, C. J., M. Vallejo-Marín, S.D. Leonhardt. *In Press*. Mutualisms and (a)symmetry in plant-
757 pollinator interactions. *Current Biology*. Whalen, M. D. 1979. Allozyme variation and evolution
758 in *Solanum* section *Androceras*. *American Society of Plant Taxonomists* 4: 203–222.
- 759 Whalen, M. D. 1978. Reproductive character displacement and floral diversity in *Solanum* section

760 *Androcera*. *Systematic Biology* 3: 77–86.

761 Zung, J. L., J. R. K. Forrest, M. C. Castellanos, and J. D. Thomson. 2015. Bee- to bird-pollination shifts
762 in *Penstemon*: effects of floral-lip removal and corolla constriction on the preferences of free-
763 foraging bumble bees. *Evolutionary Ecology* 29: 341–354.

764

765 TABLES

766 **Table 1.** POLLEN dispensing schedule metrics for six *Solanum* taxa during simulated buzz pollination. In each treatment, flowers were subjected to 30
 767 vibrations. All species were subjected to vibrations with a peak velocity of 80 mm/s and frequency of 300 Hz (which equals an acceleration of 151 m/s² and
 768 a displacement of 42 μm). Two species (*Solanum citrullifolium* and *S. heterodoxum*) were also exposed to two lower velocity vibrations, i.e., 40 mm/s
 769 (acceleration = 75 m/s²; displacement = 21 μm) and 20 mm/s (acceleration = 38m/s²; displacement = 11 um). Median ± standard error. *N* = sample size.

Species	Pollen grains per flower (x10 ³)	Frequency (Hz)	Peak velocity (mm/s)	Percentage pollen released in first vibration	Dispensing rate <i>b</i>	Percentage pollen released in 30 vibrations	<i>N</i>
Series Androceras							
(SC-SH clade)							
<i>S. citrullifolium</i>	180 ± 12	300	80	9.54 ± 2.62	0.69 ± 0.09	17.50 ± 3.33	10
		300	40	2.16 ± 2.95	0.22 ± 0.12	10.98 ± 2.00	10
		300	20	0.13 ± 0.08	0.05 ± 0.09	4.61 ± 2.08	10
<i>S. heterodoxum</i>	22 ± 2	300	80	46.03 ± 5.88	0.87 ± 0.08	61.55 ± 6.02	10
		300	40	4.81 ± 3.32	0.35 ± 0.09	17.45 ± 4.10	9
		300	20	1.31 ± 1.82	0.08 ± 0.10	7.14 ± 4.78	9
Series Pacificum							
(SR-SF clade)							
<i>S. rostratum</i>	288 ± 71	300	80	2.52 ± 0.97	0.38 ± 0.06	7.97 ± 1.55	10

<i>S. fructu-tecto</i>	76 ± 8	300	80	21.40 ± 7.33	0.60 ± 0.05	38.47 ± 10.64	5
Series Violaceiflorum							
(SGN-SGG clade)							
<i>S. grayi</i> var.	466 ± 53	300	80	0.58 ± 0.13	0.28 ± 0.08	1.77 ± 0.44	10
<i>grandiflorum</i>							
<i>S. grayi</i> var. <i>grayi</i>	113 ± 11	300	80	1.63 ± 0.55	0.35 ± 0.08	4.75 ± 1.25	10

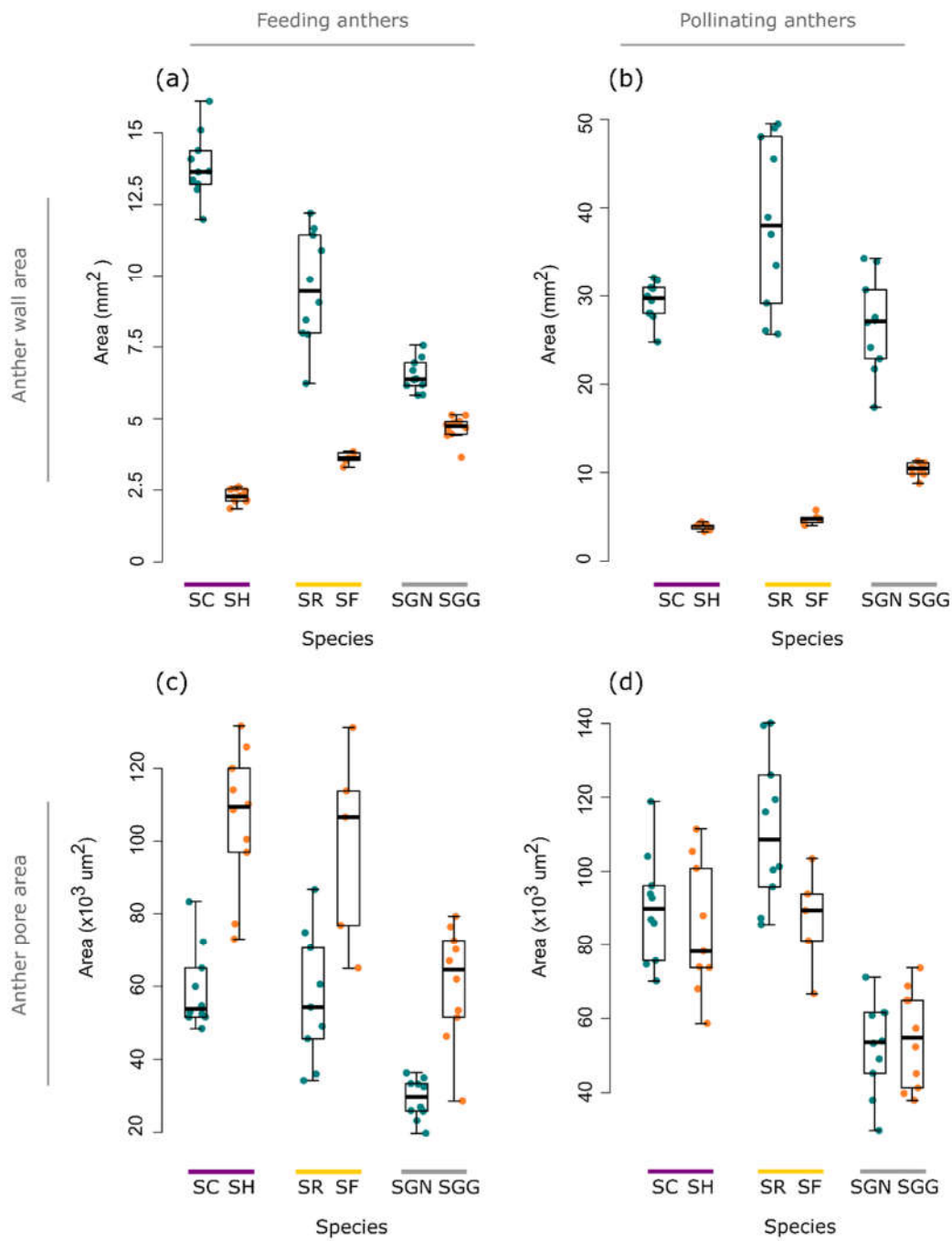
770

771 **Table 2.** ASSOCIATION between pollen dispensing schedules and various anther traits assessed using
 772 mixed-effect models. (a) Negative binomial mixed effect model with species identity as random
 773 factor. We used the number of pollen grains released in the first vibration as response variable, and
 774 tested whether this is associated with the anther wall area and anther pore area of the feeding and
 775 pollinating anthers separately. We used the total amount of pollen in a flower as offset in the model.
 776 (b) Logistic mixed-effects model with species identity as random factor. We used untransformed
 777 pollen dispensing rates (*b*; ranging from 0 to 1) as response variable (with high values indicating
 778 most pollen is released in few vibrations) and tested whether this was associated with the anther
 779 wall area and anther pore area of the feeding and pollinating anthers separately. Significance at $P <$
 780 0.05 is indicated in bold.

(a) Pollen released in first vibration			
Variable	Coefficient	SE	<i>P</i> -value
Intercept	-3.2191	0.8657	
<i>Feeding anther:</i>			
Area (mm ²)	0.0299	0.0319	0.35
Pore size (mm ²)	2.1685	1.7722	0.22
<i>Pollinating anther:</i>			
Area (mm ²)	-0.0751	0.0336	0.03
Pore size (mm ²)	5.4196	4.3688	0.21
(b) Pollen dispensing rate (<i>b</i>)			
Fixed effect	Coefficient	SE	<i>P</i> -value
Intercept	-0.2263	1.2193	
<i>Feeding anther:</i>			
area	0.0471	0.0313	0.13
pore size	0.3294	4.0790	0.94
<i>Pollinating anther:</i>			
area	-0.0973	0.0499	0.05
pore size	8.8027	16.7648	0.60

781

782



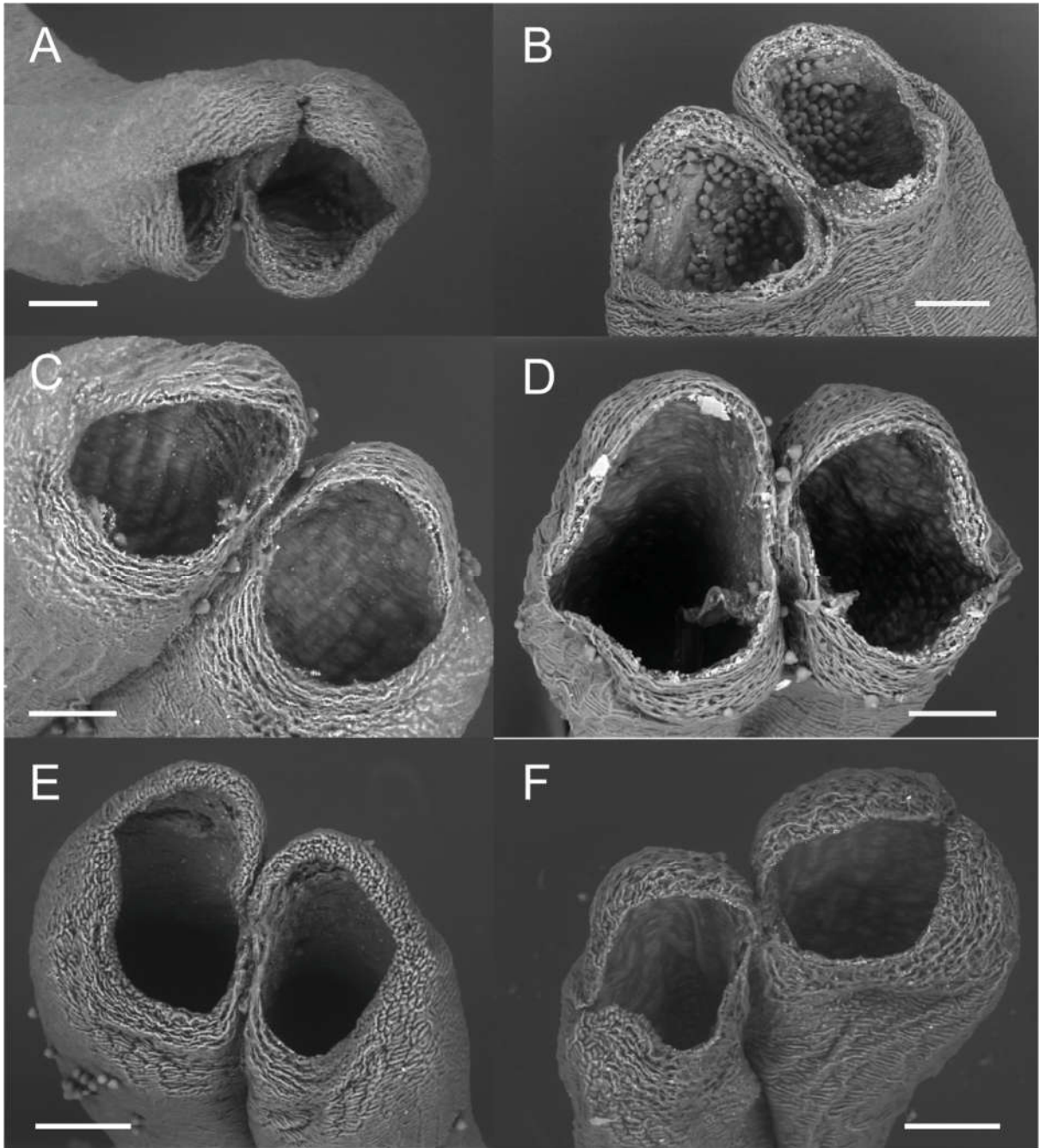
784

785

786 **Figure 1.** Anther wall (top panel) and anther pore areas (bottom panel) for the feeding (lefthand
 787 panel) and pollinating (righthand panel) anthers of three pairs of taxa in *Solanum* section *Androceras*
 788 (*Solanaceae*). Anther wall area was calculated following Buchmann and Hurley (1978) as the product
 789 of the length and breadth of anthers. Anther pore area was measured from SEM photographs. We

790 show the values of individual anthers, and not the summed values used in the analyses. The six
791 studied taxa belong to three phylogenetic clades indicated by the purple, yellow and grey lines
792 above taxon names. Within each clade, blue dots indicate the large-flowered type and orange dots
793 indicate the small-flowered type. Species names are: SC = *Solanum citrullifolium*; SH = *S.*
794 *heterodoxum*; SR = *rostratum*; SF = *S. fructu-tecto*; SGN = *S. grayi* var. *grandiflorum*; SGG = *S. grayi*
795 var. *grayi*.

796



797

798

799

800

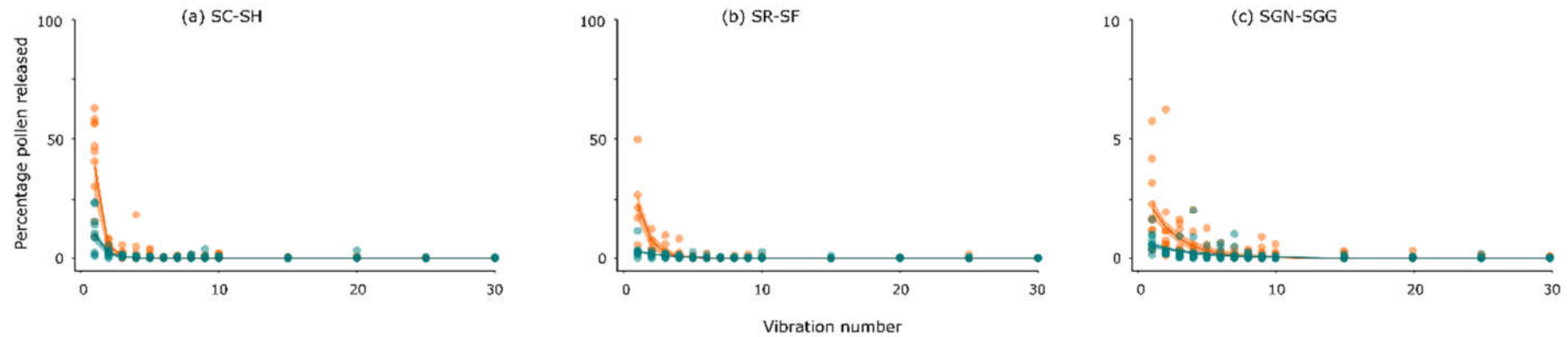
801

802

803

Figure 2. Pores of the pollinating anthers of (A) *Solanum rostratum*, (B) *S. fructu-tecto*, (C) *S. citrullifolium*, (D) *S. heterodoxum*, (E) *S. grayi* var. *grandiflorum*, and (F) *S. grayi* var. *grayi*. The panel on the left represent species of the “large flower” type, and the panel on the right shows species of the “small flower” type.

804

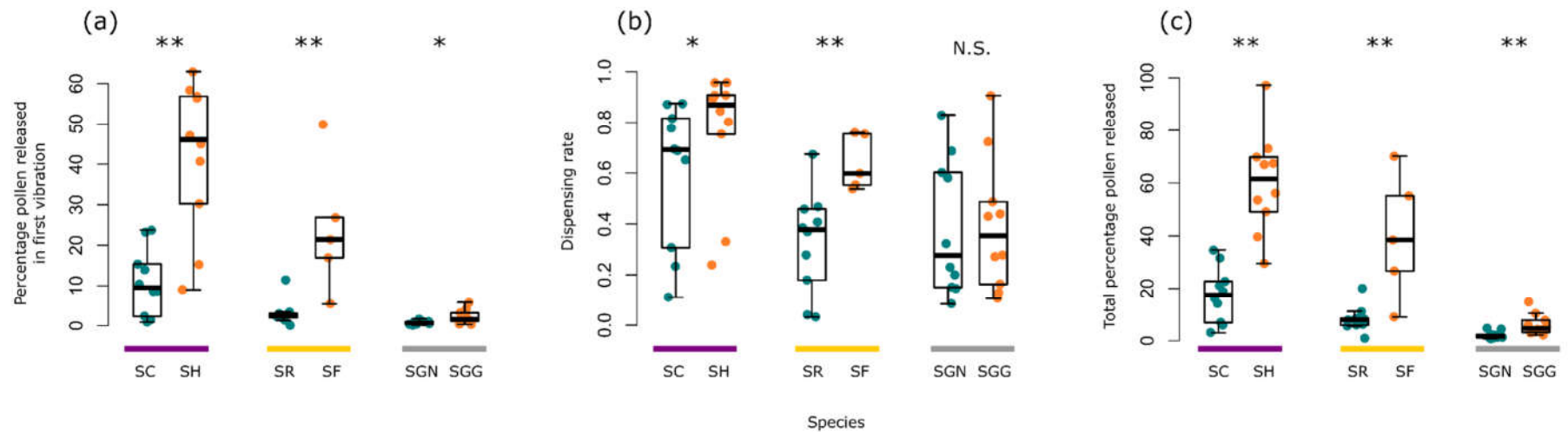


805

806

807 **Figure 3.** Pollen dispensing curves for three pairs of taxa in *Solanum* sect. *Androceras*, belonging to three phylogenetic clades: (a) Series *Violaceiflorum* (b)
808 Series *Androceras*, and (c) Series *Pacificum*. Each point shows the percentage of pollen released per vibration. Orange curves show the small flower type,
809 and blue curves show the large flower type. These curves were fitted using *nls* in R and are based on the combined data of all flowers of a species.
810 Confidence intervals (95%) were fitted using *predictNLS*. Species names as in Figure 1.

811

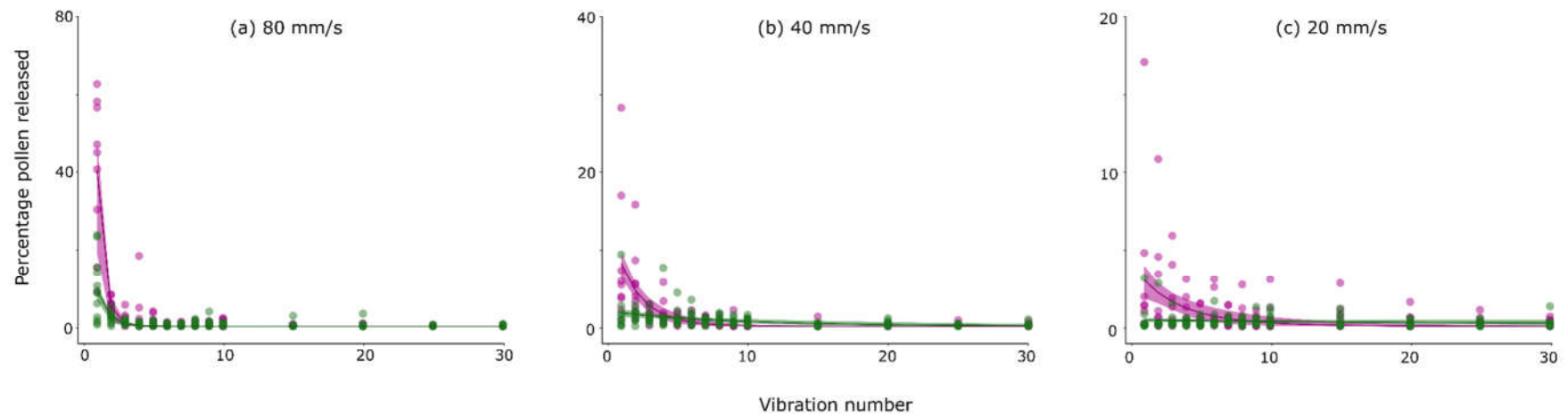


812

813

814 **Figure 4.** (a) The percentage pollen released in the first vibration is compared between flower types within the three clades, indicated by the purple, yellow
 815 and grey lines. For all clades, the small flower type released more pollen in the first vibration than the large flower type. (b) The dispensing rate is compared
 816 between flower types within the three clades. For two clades, the small flower type released pollen faster than the large flower type. (c) The total
 817 percentage pollen released across 30 vibrations is compared between flower types within clades. For all clades, the small flower type released more of its
 818 pollen than the large flower type. Orange curves show the small flower type, and blue curves show the large flower type. Species names as in Figure 1. *
 819 $0.01 < p < 0.05$; ** $0.001 < p < 0.01$.

820

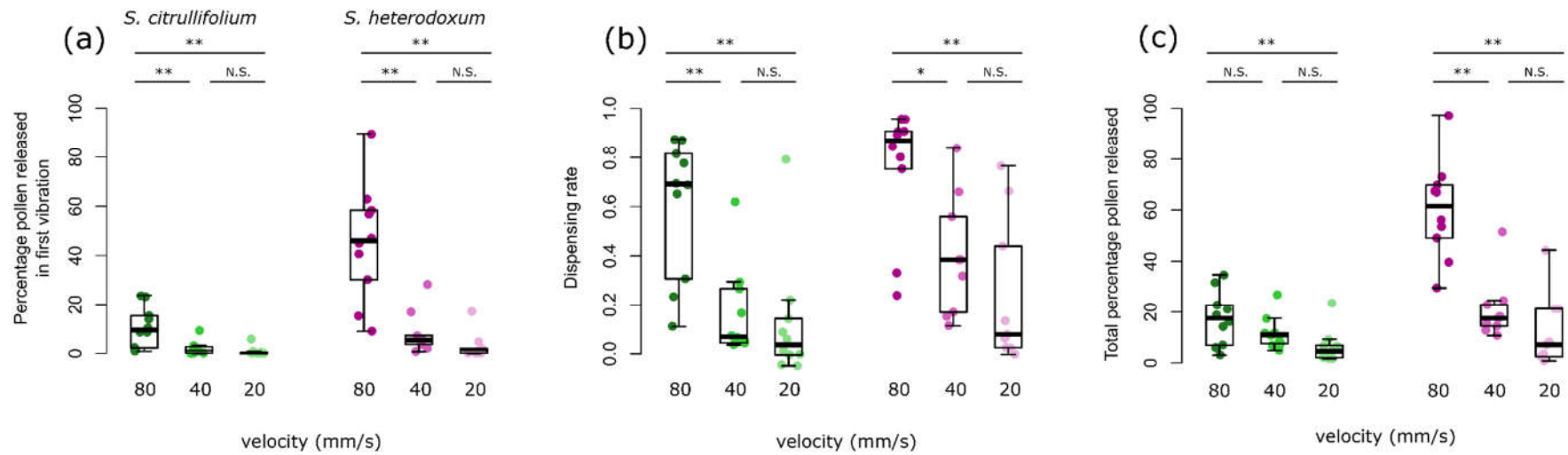


821

822

823 **Figure 5.** Pollen dispensing curves for *Solanum citrullifolium* (in green; large flower type) and *S. heterodoxum* (in pink; small flower type) when (a) 80 mm/s,
 824 (b) 40 mm/s, and (c) 20 mm/s vibration velocities were applied to flowers. Each point shows the percentage of pollen released per vibration. These curves
 825 were fitted using *nls* in R and are based on the combined data of all flowers of a species. Confidence intervals (95%) were fitted using *predictNLS*.

826



827

828

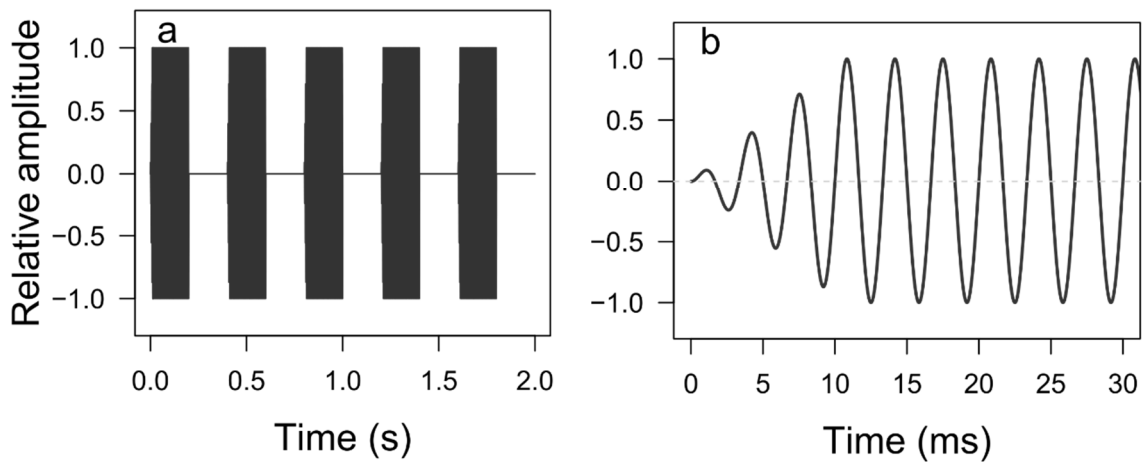
829 **Figure 6.** The percentage pollen released in the first vibration (a), the dispensing rate (b), and the total percentage pollen released across 30 vibrations (c)
 830 are compared between vibration velocities for *S. citrullifolium* (in green; large flower type) and *S. heterodoxum* (in pink; small flower type). * 0.01 < p <
 831 0.05; ** 0.001 < p < 0.01.

832 **Appendix S1.** Plant material of *Solanum* section *Androceras* used in this study.

Accession number	Species	Section	Population name	Latitude (N)	Longitude (W)
199-7-3	<i>S. citrullifolium</i>	Violaceiflorum	Nijmegen Collection	-	-
11-PTEM-14, 15	<i>S. heterodoxum</i>		Teotihuacán, Estado de México	19.68	98.84
10-s-81, 82, 86	<i>S. rostratum</i>	Androceras	San Miguel de Allende, Querétaro	20.90	100.45
10-AH-9, 24	<i>S. fructu-tecto</i>		Atitalaquia, Hidalgo	20.06	99.21
08-s-78, 79	<i>S. grayi</i> var. <i>grandiflorum</i>	Pacificum	Tejupilco, Estado de México	18.85	100.13
07-s-194b, 195b, 196b	<i>S. grayi</i> var. <i>grayi</i>		Los Álamos, Sonora	27.00	108.93

833

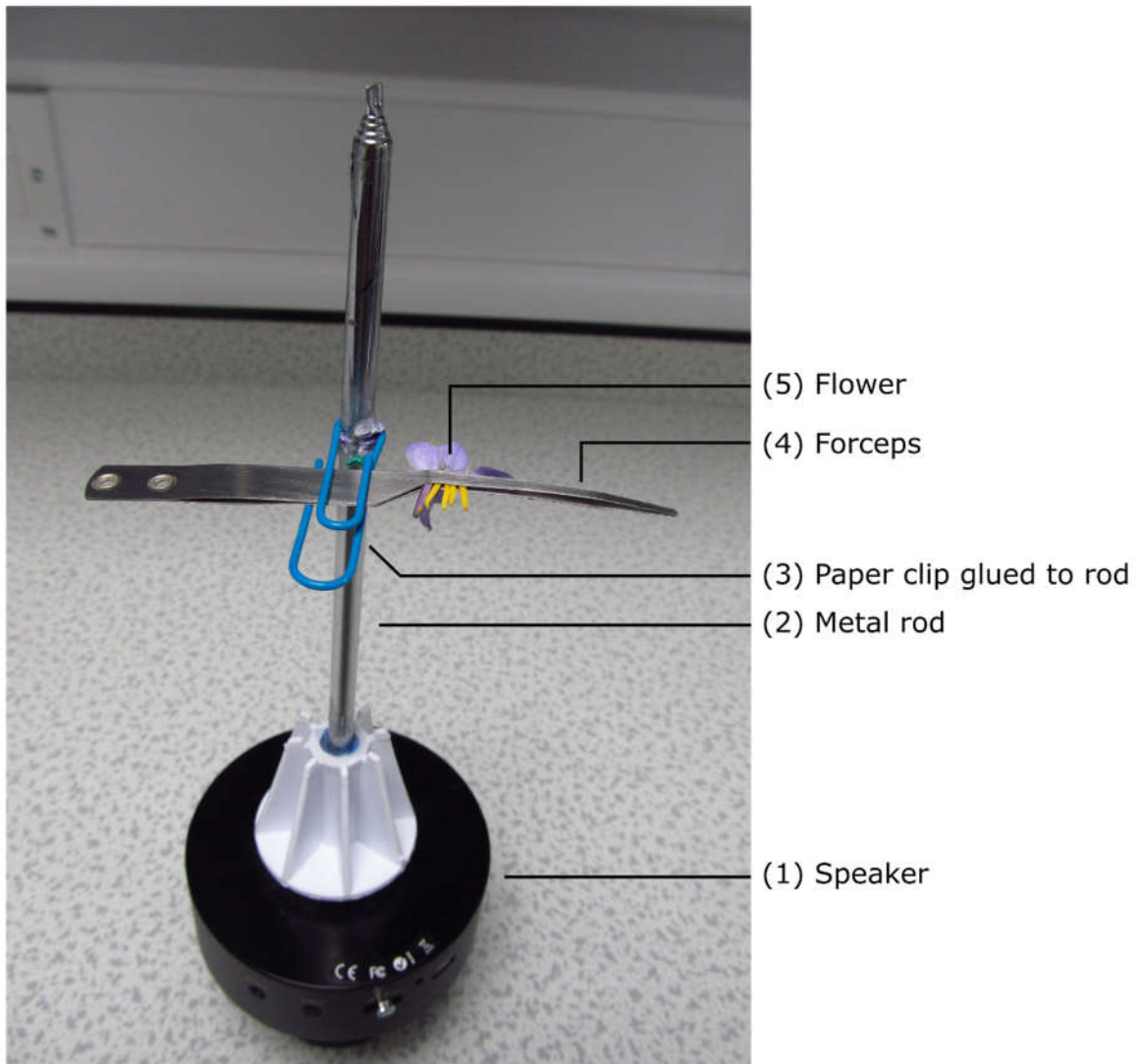
834 **Appendix S2.** Artificial vibrations applied to anthers. (a) Each stimulus consisted of five short
835 vibration pulses of 0.2 s long, with 0.2 s of silence between pulses. (b) The beginning of each 0.2 s
836 pulse consisted of a short fade-in, which is similar to what bees produce and it ensures that the
837 wave is transmitted in the expected manner.



838

839

840 **Appendix S3.** The custom-made vibration transducer system. Vibrations were transferred from a
841 laptop to (1) a speaker. From there, vibrations were transferred to (2) a metal rod that was attached
842 in the speaker with glue. Vibrations then travelled from the rod through (3) a metal clip that was
843 tightly attached to the metal rod and fixed using glue. From there, vibrations were transferred to (4)
844 forceps, and then to (5) anthers. The anthers were clasped approximately where a bee would attach.
845 Please note that in our experiments, we used storkbill short blunt forceps (D4045, Watkins &
846 Doncaster, UK) and not the long-pronged forceps depicted here.

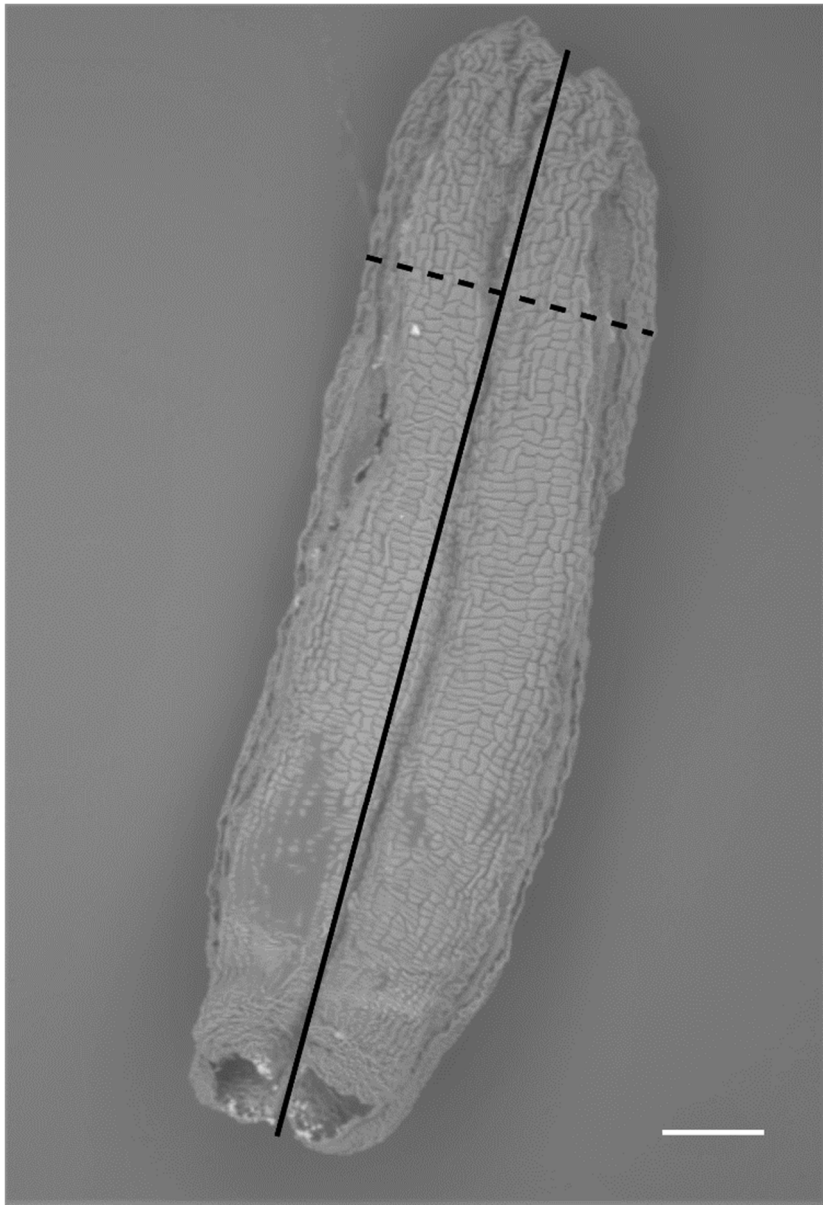


847

848

849

850 **Appendix S4.** For each anther, the length (solid line) and breadth (dashed line) was measured. For
851 each anther type within a flower the pore area was measure for one feeding and one pollinating
852 anther. The photo shows a SEM image of a *Solanum fructu-tecto* feeding anther. The scale bar
853 represents 200 μm .



854

855

856